

Chapter 2.6.2

FAST AND SLOW COLLISIONS OF IONS, ATOMS AND MOLECULES

C. D. Lin

Department of Physics,
Kansas State University,
Manhattan, Kansas 66506-2601,
U.S.A.

F. Martín

Departamento de Química, C-9,
Universidad Autónoma de Madrid,
28049-Madrid,
Spain

SCATTERING IN MICROSCOPIC PHYSICS AND CHEMICAL PHYSICS

Atomic and Molecular Scattering, Introduction to Scattering in Chemical Physics

Contents

§ 1	Introduction	1
§ 2	Time-Independent Methods	2
	The Hamiltonian and the Coordinate Systems	2
	Close-Coupling or Coupled-Channel Methods	2
	Molecular Orbital Expansion Method	3
	Hyperspherical Approach	3
§ 3	Time-Dependent Approaches	5
	The Molecular Close-Coupling Method	5
	Direct Integration of the Time-Dependent Schrödinger Equation	7
	Perturbation Approaches	8
	Relativistic Ion–Atom Collisions	9
§ 4	Atomic Collisions with Multielectron Targets	10
§ 5	Penning Ionisation and Associative Ionisation	11
§ 6	Ion–Molecule Collisions	13
	Quantum Mechanical Approach	14
	Semiclassical Approach	14
§ 7	Ion–Cluster Collisions	15
	Jellium Models	16
	Beyond the Jellium Approximation	17

§ 1. Introduction

This chapter is concerned with the electronic transitions in two-body collisions between ions, atoms and molecules. The collision energy covered ranges from the subthermal regime (less than millielectronvolts) in ion traps to the relativistic regime (greater than gigaelectronvolts) in relativistic heavy-ion colliders. Experimentally a scattering event consists of (1) the preparation of projectiles and targets in well-defined initial quantum states before the collision and (2) the determination of quantum states of the collision products at the end of the collision.

Elementary collisions involving atoms, ions and molecules occur in many gaseous and plasma environments, such as in the upper atmosphere and in gaseous discharges. Collisions of ions with atoms and/or molecules provide the heating and cooling mechanisms for the laboratory and astrophysical plasmas. Understanding the energy transfer in collisions between ions with matter and with biological molecules is essential to cancer therapy. At the fundamental level, atomic collisions provide a more efficient means for populating excited species than photons and electrons. Furthermore simple atomic collisions offer a fertile ground for testing the quantum mechanical scattering theory. This chapter addresses the application of scattering theory to solve problems in fast and slow collisions of atoms, ions and molecules.

In discussing atomic scattering theory, it is impossible not to mention the experimental progress. In the past few decades, technology has improved drastically such that experimentalists can now control beams of atoms, ions and molecules with much ease, over an ever-increasing range of energies. For example, in the 1960s, multiply charged ions were produced only at Van der Graaf accelerator or cyclotron facilities, which tend to have higher energies ranging from hundreds of kiloelectronvolts per atomic mass unit to hundreds of megaelectronvolts per atomic mass unit. In the 1980s, new ion sources such as ECR and EBIS produced multiply charged ions from fractional to tens of kiloelectronvolts per atomic mass unit. Since the 1990s, heavy-ion storage rings, combined with laser or electron cooling, has become available for precision experiments.

While most of the targets are prepared in the ground state in a collision experiment, in many applications it is desirable to prepare targets in the excited states. Such excited states have been obtained using laser excitations and the states can be oriented

or aligned using circular- or linear-polarised light, respectively. Collisions with Rydberg atoms have also been investigated.

For the collision products, the identification of excitation, charge transfer or ionisation processes can be carried out by measuring the charge states of the collision products. To determine the specific final states, methods such as photon emission, energy loss or energy gain of projectiles and selective laser excitations of collision products have been used. For multielectron systems, Auger electron emission or X-ray emission can be used to identify the final states. For ionisation processes, electron spectrometers with ever-improving resolution have been developed. In recent years, the two-dimensional momentum distributions of the recoil ions and of the ejected electrons have been measured directly. To achieve superb resolution for the recoil ions, the target atoms are supersonically cooled. In the future they can be prepared by laser cooling as well.

The rest of this chapter is organised as follows. The next three sections address the basic theoretical issues and approximations for ion–atom collisions. §5–§7 discuss theories for Penning ionisation, associative ionisation and ion–molecule and ion–cluster collisions.

§2. Time-Independent Methods

The Hamiltonian and the Coordinate Systems

Consider a prototype ion–atom collision system where a bare ion A^+ impinges on a one-electron atom ($B^+ + e^-$). Within the nonrelativistic theory, the collision dynamics is governed by the time-independent Schrödinger equation

$$H\psi = E\psi, \quad (1)$$

where H is the Hamiltonian and E is the total energy of the system.

The time-independent wave function is described by six variables in the centre-of-mass frame. In such a simple collision, the inelastic process consists of target excitation, electron capture and ionisation processes. At low energies the ionisation process is not important. In Fig. 1 three sets of Jacobi coordinates that can be used to solve Eq. (1) are shown. In Jacobi coordinates, the kinetic energy operator for the three particles is separable

$$T_i = -\frac{1}{2m_i} \nabla_{\mathbf{r}_i}^2 - \frac{1}{2\mu_i} \nabla_{\mathbf{R}_i}^2, \quad (2)$$

where $i = \alpha, \beta, \gamma$. In the equation above and the rest of this chapter, atomic units ($m_e = \hbar = e = 1$) are used throughout unless otherwise noted. The reduced masses in this equation depend on the coordinate system used. In terms of the masses of the three particles, M_A , M_B and $m (=1$ for the electron), the reduced masses entering Eq. (2) for the α set, for example, are

given explicitly by

$$m_\alpha = \frac{M_A + M_B}{M_A + M_B + 1}; \quad \mu_\alpha = \frac{M_A M_B}{M_A + M_B} = \mu, \quad (3)$$

where μ is defined to be the reduced mass of the two heavy particles. The reduced masses for the β and the γ set of coordinate frames are similarly defined. If non-Jacobi coordinates are used, such as the last system shown in Fig. 1, the kinetic energy operator T becomes

$$T = -\frac{1}{2m} \nabla_{\mathbf{r}}^2 - \frac{1}{2\mu} \nabla_{\mathbf{R}}^2 - \frac{1}{M} \nabla_{\mathbf{R}} \cdot \nabla_{\mathbf{r}}, \quad (4)$$

where the last term is nondiagonal, and is known as the mass polarisation term. In this coordinate system where O is an arbitrary point, $OA = pR$, $OB = qR$ with $p + q = 1$, the various masses are given by

$$m = \frac{m_\alpha \mu}{m_\alpha \Delta^2 + \mu}, \quad M = \frac{\mu}{\Delta}, \quad \Delta = \frac{pM_A - qM_B}{M_A + M_B}. \quad (5)$$

The potential energy entering the Schrödinger equation is very simple in general. It is the sum of the pair-wise Coulomb interactions.

Close-Coupling or Coupled-Channel Methods

A general approach to solve the multidimensional partial differential equation (1) is the close-coupling method (Bransden and McDowell, 1992; Fritsch and Lin, 1991). Consider direct excitation and electron capture processes only. The solution of Eq. (1) can be expanded as

$$\psi = \sum_{j=1}^M X_j(\mathbf{R}_\beta, \mathbf{r}_\beta) F_j(\mathbf{R}_\beta) + \sum_{j=M+1}^N Y_j(\mathbf{R}_\gamma, \mathbf{r}_\gamma) G_j(\mathbf{R}_\gamma), \quad (6)$$

where X_j and Y_j are the channel functions. They reduce to the bound states of the two-body systems in the asymptotic region,

$$X_j(\mathbf{R}_\beta, \mathbf{r}_\beta) \xrightarrow{R_\beta \rightarrow \infty} \phi_j(\mathbf{r}_\beta) \quad (7)$$

$$Y_j(\mathbf{R}_\gamma, \mathbf{r}_\gamma) \xrightarrow{R_\gamma \rightarrow \infty} \chi_j(\mathbf{r}_\gamma),$$

where ϕ_j and χ_j are the bound states of the ($e^- + B^+$) system and the ($e^- + A^+$) system, respectively. Eq. (6) when substituted (6) into Eq. (1) and the variational procedure is used, a set of coupled integrodifferential equations for $F_j(\mathbf{R}_\beta)$ and $G_j(\mathbf{R}_\gamma)$ is obtained, which is exact for any three-body system except for the basis set truncation. For example, the resulting equations can be used to study positron–hydrogen atom collisions; see Chapter 2.6.1. The essential approximation for ion–atom collision theory is to take advantage of the fact that the mass of each of the heavy particles is much larger than the mass of the electron and to use this fact to simplify the resulting close-coupling equations. From the geometries in Fig. 1, the two radius vectors in the γ set are related to the two vectors in the β set by

$$\mathbf{r}_\gamma = -\mathbf{R}_\beta + \frac{M_B}{M_B + 1} \mathbf{r}_\beta \cong -\mathbf{R}_\beta + \mathbf{r}_\beta \quad (8)$$

$$\mathbf{R}_\gamma = \frac{M_A}{M_A + 1} \mathbf{R}_\beta + \frac{M_A + M_B + 1}{(M_A + 1)(M_B + 1)} \mathbf{r}_\beta = \mathbf{R}_\beta + \frac{1}{\mu} \mathbf{r}_\beta,$$

where the fact that M_A and M_B are much larger than 1 has been used. This allows one to write

$$G_j(\mathbf{R}_\gamma) = G_j(-\mathbf{R}_\beta + \frac{1}{\mu} \mathbf{r}_\beta) = T(\frac{1}{\mu} \mathbf{r}_\beta) G_j(\mathbf{R}_\beta), \quad (9)$$

where T is the translation operator, $T(\mathbf{x}) = \exp[i P_{\mathbf{R}_\beta} \cdot \mathbf{x}]$. For collisions at energies above hundreds of electronvolts, G_j is a sharply peaked function in the direction of the incident ion at large internuclear separations, so that it is possible to approximate (9) by

$$G_j(\mathbf{R}_\gamma) \cong e^{i\mathbf{v}_j \cdot \mathbf{r}_\beta} G_j(\mathbf{R}_\beta), \quad (10)$$

where the phase factor is often called the electron translational factor, with \mathbf{v}_j being approximately equal to the velocity of the ion.

Molecular Orbital Expansion Method

Intuitively, the ion–atom collision complex at low energies can be approximated as a transient molecule where the electronic motion is separated from the nuclear motion. The electronic wave function is obtained by solving

$$\left[-\frac{1}{2} \nabla_{\mathbf{r}}^2 + V - E_n(R) \right] \varphi_n(\mathbf{r}; \mathbf{R}) = 0 \quad (11)$$

at a fixed internuclear distance R , where V is the potential seen by the electron. Note that the molecular frame coordinates are used (the α set) in (11) but the indices have been suppressed. Each molecular orbital $\varphi_n(\mathbf{r}; \mathbf{R})$ separates into an atomic orbital on atom A or atom B at large internuclear distances. Using these molecular orbitals, one can expand

$$\psi = \sum_n F_n(\mathbf{R}) \varphi_n(\mathbf{r}; \mathbf{R}). \quad (12)$$

After multiplying the Schrödinger equation $(H - E)\psi = 0$ by φ_n^* and integrating over the electronic coordi-

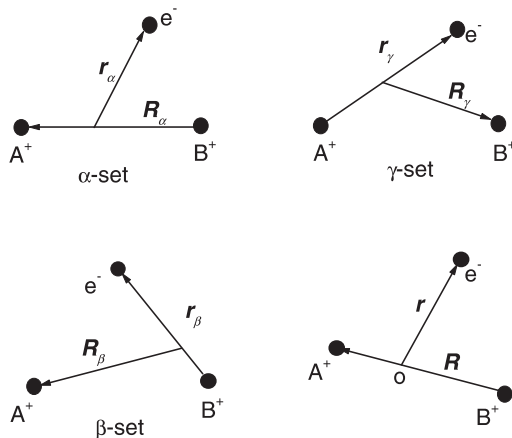
nates, one obtains a set of coupled-channel equations for $F_n(\mathbf{R})$,

$$\begin{aligned} & \left[-\frac{1}{2\mu} \nabla_{\mathbf{R}}^2 + E_n(\mathbf{R}) - E \right] F_n(\mathbf{R}) \\ & = \frac{1}{2\mu} \sum_k \left\langle \varphi_n \left| \frac{\partial^2}{\partial R^2} \right| \varphi_k \right\rangle F_k(\mathbf{R}) \\ & + \frac{1}{\mu} \sum_k \langle \varphi_n | \nabla_{\mathbf{R}} | \varphi_k \rangle \nabla_{\mathbf{R}} F_k(\mathbf{R}). \end{aligned} \quad (13)$$

The brackets denote integration over the electron coordinates. Equation (13) is commonly known as the perturbed stationary state (PSS) approximation. With proper generalisation to many-electron wave functions, the PSS approximation has been widely used for treating ion–atom and atom–atom collisions since its first introduction by Massey and Smith (1933). However, the asymptotic wave functions in the PSS approximation do not satisfy the correct boundary conditions. This deficiency results in a number of problems in practical applications. First the coupling matrix elements in (13) depend on the choice of the origin for the electron coordinates. Second, the coupling matrix elements may remain nonzero as the internuclear distance goes to infinity, suggesting that the PSS model may predict unphysical transitions at large internuclear separations (Delos, 1981).

For collisions at higher energies, say on the order of kiloelectronvolts per atomic mass unit, the motion of the heavy particles can be described classically. A commonly used remedy to this approximation is to introduce electron translational factors where each molecular orbital in (12) is multiplied by a phase factor, $\exp[i\mathbf{v} \cdot \mathbf{r}f(\mathbf{R}, \mathbf{r})]$, where different forms of $f(\mathbf{R}, \mathbf{r})$ have been used. The electron translational factors are not valid in the low-energy region where inelastic collision requires a full quantum-mechanical treatment. One useful approach that can be used for low-energy ion–atom collisions without all the problems of the perturbed stationary state approximation is the hyperspherical approach.

Figure 1 Three sets of Jacobi coordinates and one non-Jacobian coordinates for three particles.



Hyperspherical Approach

The fundamental difficulties of the PSS model can be avoided if one formulates ion–atom collisions within the framework of the hyperspherical approach (Lin, 1995). Starting with any one of the three Jacobi coordinate systems as in Fig. 1, one can define two mass-weighted vectors

$$\begin{aligned} \xi_1 &= \sqrt{\frac{\mu_1}{\mu}} \mathbf{r}_1 \\ \xi_2 &= \sqrt{\frac{\mu_2}{\mu}} \mathbf{r}_2, \end{aligned} \quad (14)$$

where μ is an arbitrary scaling mass and \mathbf{r}_1 and \mathbf{r}_2 are the pair of radius vectors of any set of Jacobi coordinates in Fig. 1, with reduced masses μ_1 and μ_2 ,

respectively. Introducing the hyperradius ρ and the hyperangle ϕ through

$$\begin{aligned}\rho &= \sqrt{\xi_1^2 + \xi_2^2} \\ \tan \phi &= \xi_2 / \xi_1,\end{aligned}\quad (15)$$

the Schrödinger equation is given by

$$\left(-\frac{1}{2\mu} \frac{\partial^2}{\partial \rho^2} + \frac{\Lambda^2 - \frac{1}{4}}{2\mu\rho^2} + V(\rho, \phi, \theta) \right) \psi = E\psi, \quad (16)$$

where θ is the angle between ξ_1 and ξ_2 and

$$\Lambda^2 = -\frac{\partial^2}{\partial \phi^2} + \frac{\varrho_1^2(\hat{\xi}_1)}{\cos^2 \phi} + \frac{\varrho_2^2(\hat{\xi}_2)}{\sin^2 \phi} \quad (17)$$

is the grand angular momentum operator with ϱ_i being the orbital angular momentum operator associated with the radius vector ξ_i . The hyperradius ρ is invariant for all the three Jacobi coordinates, but the remaining five hyperspherical angles $\Omega = (\phi, \xi_1, \xi_2)$ depend on the specific Jacobi coordinates. However, $\Lambda^2(\Omega^\alpha) = \Lambda^2(\Omega^\beta) = \Lambda^2(\Omega^\gamma)$. Equation (16) can be solved in the same fashion as the Born–Oppenheimer approximation with ρ being treated as the slow variable,

$$\psi = \sum_{\mu} F_{\mu}(\rho) \Phi_{\mu}(\rho; \Omega), \quad (18)$$

where the channel functions $\Phi_{\mu}(\rho; \Omega)$ are obtained by solving

$$\left[\frac{\Lambda^2 - \frac{1}{4}}{2\mu\rho^2} + V(\rho, \theta, \phi) \right] \Phi_{\mu}(\rho; \Omega) = U_{\mu}(\rho) \Phi_{\mu}(\rho; \Omega). \quad (19)$$

The set of hyperspherical potential curves $U_{\mu}(\rho)$ is analogous to molecular potential curves in the Born–Oppenheimer approximation. In the limit of large ρ , each low-energy channel function dissociates into a two-body bound state.

Equation (19) can be solved in the body frame similar to the Born–Oppenheimer approach as well. In the α -set coordinates, define the body-frame z' axis to be along ξ_1 , the y' axis perpendicular to the plane formed by the three particles and x' given such that the body-frame (x', y', z') axes form a right-handed orthogonal set. The Euler angles of the body frame are $\omega = (\omega_1, \omega_2, \omega_3)$ with $\omega_2 = \theta_1$, $\omega_1 = \phi_1$, where (θ_1, ϕ_1) are the spherical angles of ξ_1 . In the body frame the total wave function can be expanded as

$$\psi(\rho, \Omega) = \sum_{\mu} \sum_I F_{\mu I}(\rho) \Phi_{\mu I}(\rho; \theta, \phi) \bar{D}_{IM_J}^J(\omega_1, \omega_2, \omega_3), \quad (20)$$

where \bar{D} is the symmetrized Wigner D function, J is the total angular momentum, I and M_J are the projections along the body-frame and the laboratory-frame quantisation axes, respectively.

This expansion is very similar to the perturbed stationary state approximation in the body-frame where

the “channel function” $F_{\mu I}(\rho)$ is the solution of

$$\begin{aligned}\left(-\frac{\partial^2}{\partial \rho^2} - \frac{1}{4\rho^2} - 2\mu E \right) F_{\mu I}(\rho) + \sum_{\nu I'} [V_{\mu I, \nu I'}(\rho) \\ + W_{\mu I, \nu I'}(\rho)] F_{\nu I'}(\rho) = 0,\end{aligned}\quad (21)$$

where

$$\begin{aligned}V_{\mu I, \nu I'}(\rho) &= \langle \Phi_{\mu I}(\rho; \theta, \phi) \bar{D}_{IM_J}^J | \Lambda^2 + 2\mu V | \\ &\Phi_{\nu I'}(\rho; \theta, \phi) \bar{D}_{I'M_J}^J \rangle,\end{aligned}\quad (22)$$

which includes the rotational coupling terms, and

$$\begin{aligned}W_{\mu I, \nu I'}(\rho) &= 2 \left\langle \Phi_{\mu I}(\rho; \theta, \phi) \left| \frac{d}{d\rho} \right| \Phi_{\nu I'}(\rho; \theta, \phi) \right\rangle \frac{d}{d\rho} \\ &+ \left\langle \Phi_{\mu I}(\rho; \theta, \phi) \left| \frac{d^2}{d\rho^2} \right| \Phi_{\nu I'}(\rho; \theta, \phi) \right\rangle\end{aligned}\quad (23)$$

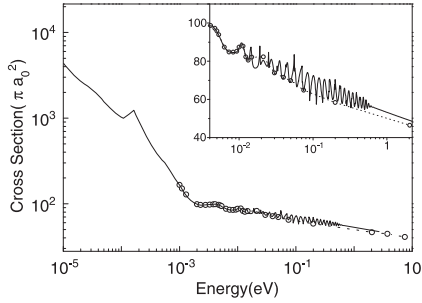
gives the radial coupling terms.

It is well known from the PSS approximation that the radial coupling terms are difficult to evaluate accurately in the region where the potential curves show avoided crossings. In recent years there have been different proposals to deal with these sharp avoided crossings. One is the so-called diabatic-by-sector method. In this method the hyperradius is divided into many small sectors and the channel functions $\Phi_{\mu I}(\rho; \theta, \phi)$ are fixed within each sector such that there is no $W_{\mu I, \nu I'}(\rho)$ coupling terms. Within each sector the coupled differential equations are integrated from the beginning to the end of the sector where the total hyperradial wave function and its derivative are matched to the respective functions in the next sector. This procedure is continued till the large R region where they are matched to the asymptotic solutions in the laboratory frame (Lin, 1995). Another method is the so-called slow-variable method (Tolstikhin *et al.*, 1996). These approaches are much easier to implement when many channels are included in the calculations.

The hyperspherical approach outlined above (Lin, 1995) is useful for any three-body collision systems. It has not been widely used in ion–atom collisions since many partial waves are needed in such systems. However, it has been shown (Igarashi and Lin, 1999) recently that a procedure similar to the PSS approximation can be used for applying the hyperspherical method to ion–atom collisions; i.e., the potential curves and coupling terms must only be calculated once. This new observation makes the hyperspherical approach as easy to use as the PSS model, yet without the inherent problems associated with the PSS model. The method has been applied to obtain electron transfer cross sections for the process $D^+ + H(1s) \rightarrow D(1s) + H^+$ and the results are shown in Fig. 2. Note that the cross section shows interesting structures at low energies. We comment that the standard PSS model cannot handle this process since the

isotope effect is not included in that model. However, with special treatments the PSS model can be modified to describe this process except close to the threshold.

Figure 2 Charge transfer cross sections for $D^+ + H(1s) \rightarrow D(1s) + H^+$ collisions at low energies calculated using the hyperspherical approach. Taken from Igarashi and Lin (1999).



§3. Time-Dependent Approaches

In the time-independent approach for describing ion-atom or ion-molecule collisions it is necessary to employ partial wave expansion in order to obtain the scattering cross sections. Even at thermal energies the number of partial waves needed for a converged calculation easily runs into several thousands. For collision energies greater than a few kiloelectronvolts per atomic mass unit it is possible to treat the motion of the heavy particles classically. The electron is moving in the field of a time-dependent potential and its motion is governed by the time-dependent Schrödinger equation

$$H_{el}\phi(\mathbf{r};\mathbf{R}) = i(\partial/\partial t)\phi(\mathbf{r};\mathbf{R}), \quad (24)$$

where H_{el} is the electronic Hamiltonian. Thus in the time-dependent approach, the goal is to solve Eq. (24) to extract the electronic transition probability $P_i(b)$ for each impact parameter b . The total cross section is obtained by integrating the probabilities over the impact parameter plane.

The Molecular Close-Coupling Method

The time-dependent Schrödinger equation (24) can be solved by expanding in a basis set

$$\phi(\mathbf{r}, t) = \sum_s a_s(t) \phi_s(\mathbf{r}, t) \exp\left(-i \int^t E_s(t') dt'\right), \quad (25)$$

where ϕ_s has energy eigenvalues E_s , and the functions form an orthonormal complete set at each internuclear separation $\mathbf{R}(t)$. From (24) and (25) one can obtain a set of coupled equations for $a_n(t)$:

$$i \dot{a}_n(t) = \sum_s a_s(t) \langle \phi_n | H_{el} - i d/dt | \phi_s \rangle > \exp\left\{-i \int^t (E_s - E_n) dt'\right\}. \quad (26)$$

This set of coupled equations are to be solved under proper initial conditions. It is desirable to choose basis functions that reduce to the eigenstates in the separated-atom limit. This would allow a precise specification of the initial state and $a_s(t \rightarrow \infty)$ can then be identified as the scattering amplitudes directly.

The differential operator d/dt in (26) operates in a space-fixed collision frame (x, y, z) . A convenient alternative frame is the molecular frame where z' is along the internuclear axis.

From Eq. (26) a number of analytic results can be obtained for certain two-channel models.

Two-Channel Models

The Landau-Zener Model In this model the Hamiltonian takes the form

$$H_{el} = \begin{bmatrix} H_{11} & H_{12} \\ H_{21} & H_{22} \end{bmatrix}, \quad (27)$$

where $H_{12} = H_{21}$. As a function of R , H_{11} and H_{22} cross at R_x , and in the coupling region, H_{12} is approximated as a constant. Furthermore, let $d(H_{11} - H_{22})/dt = d(\Delta E_{12})/dt = \alpha$, then the two-channel version of Eq. (26) is solved to obtain the probability for making transitions from one channel to the other. The Landau-Zener probability for making such a single transition is

$$P = e^{-2\pi j}, \quad (28)$$

where

$$j = H_{12}^2/\alpha = \frac{H_{12}^2}{|v d(\Delta E_{12})/dR|} \quad (29)$$

and $v = dR/dt$ is the relative radial velocity of the two heavy particles at R_x . In a full collision there are two possible paths for making the transition from one channel to the other and the probability is $2P(1-P)$. Thus transition is most probable when P is near $1/2$. When P is large the crossing can be treated as diabatic. When P is small, the crossing is adiabatic. If the interference between the two passages is included in the Landau-Zener model the resulting probability will show oscillations with respect to the collision velocity or the impact parameter. Such oscillations are known as Stückelberg oscillations.

The Demkov-Meyerhof Model This model is useful when two channels are nearly degenerate in the dissociation limit and the coupling between the two channels is $H_{12} = \beta \exp(-\alpha t)$. The probability for making the transition between the two channels is

$$P = \text{sech}^2 \left\{ \frac{\pi \Delta E_{12}}{2\alpha} \right\} \sin^2 \left\{ \int H_{12} dt \right\}, \quad (30)$$

where $\Delta E_{12} = H_{11} - H_{22}$. The oscillating sine function is due to the interference from the two paths. This result is known as the Demkov model. If a single

passage is used the probability for making the transition is

$$P_1 = (1 + e^{2x})^{-1}, \quad (31)$$

where $x = \pi\Delta E_{12}/(2\alpha)$. This is known as the Meyerhof model.

The Rotational Coupling Rotational coupling exists between two states when their magnetic quantum numbers along the internuclear axis differ by one unit. If the rotational coupling matrix element is approximated as a constant and the energy difference between them is zero, then the transition probability is calculated to be

$$P = \sin^2 \theta_0, \quad (32)$$

where θ_0 is the scattering angle.

These three simple two-channel models, together with models like the Rosen–Zener model, the Nikitin model, and the multichannel Landau–Zener model (Bransden and McDowell, 1992), have been used repeatedly to interpret qualitatively or semiquantitatively many ion–atom and atom–atom collisions in the absence of detailed dynamic calculations. On the other hand, it is desirable to perform full *ab initio* calculations to obtain inelastic scattering cross sections.

Multichannel Close-Coupling Methods In Eq. (25), it is assumed that the basis functions form an orthogonal set at each time step or at each internuclear separation. The most commonly used basis functions in actual *ab initio* calculations consist of either molecular orbitals (MO) or atomic orbitals (AO) in general. When adiabatic molecular orbitals are used, the basis functions are orthogonal and one must solve Eq. (26). However, as explained under Molecular Orbital Expansion Method, the molecular basis functions do not satisfy the asymptotic boundary conditions and switching functions must be introduced. By multiplying orbital-dependent switching functions to individual adiabatic molecular orbitals, the resulting basis functions are not orthogonal and such nonorthogonality must be taken into account in deriving the coupled equations. (Orthogonality can still be retained if a common translational factor is applied to all molecular orbitals.) Similarly, in calculations using atomic orbitals, those orbitals belonging to the different centres are not orthogonal. Thus, instead of (25), in the general close-coupling description of atomic collisions, the motion of the electron in configuration space is spanned in a finite set of nonorthogonal basis functions $\psi_k(\mathbf{r}, t)$, $k = 1, \dots, N$ (Bransden and McDowell, 1992; Fritsch and Lin, 1991). In such a truncated expansion the time-dependent electronic wave function is approximated as

$$\Psi(\mathbf{r}, t) = \sum_{k=1}^N a_k(t) \psi_k(\mathbf{r}, t) \quad (33)$$

with the time-dependent coefficients $a_k(t)$. Instead of (26), the system of coupled equations is

$$\sum_{k=1}^N N_{jk}(t) \frac{da_k(t)}{dt} = i \sum_{k=1}^N M_{jk}(t) a_k(t), \quad j = 1, \dots, N \quad (34)$$

from which the amplitudes can be solved. This equation contains the overlap matrix elements $M_{jk}(t) = \langle \psi_j | \psi_k \rangle$ and the coupling matrix elements $N_{jk}(t) = \langle \psi_j | i(\partial/\partial t) - H_{el} | \psi_k \rangle$. In the case of the AO expansion, the basis functions for the bound states in atomic centres *A* and *B* are chosen to have the correct asymptotic form

$$\begin{aligned} \psi_k^A(\mathbf{r}, t) &= \phi_k^A(r_A) \exp\left(iv_A \cdot \mathbf{r} - \frac{1}{2}i \int^t dt' v_A^2 - i\epsilon_k^A t\right), \\ \psi_k^B(\mathbf{r}, t) &= \phi_k^B(r_B) \exp\left(iv_B \cdot \mathbf{r} - \frac{1}{2}i \int^t dt' v_B^2 - i\epsilon_k^B t\right), \end{aligned} \quad (35)$$

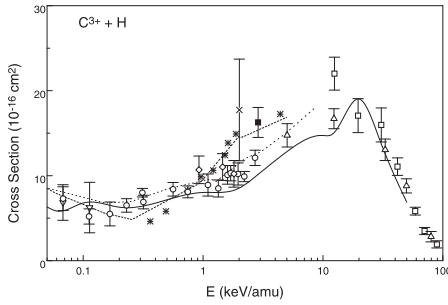
where ϕ_k^i and ϵ_k^i ($i = A, B$) are the eigenstates and the eigenenergies of the atomic states on centre *i*. Note that plane-wave electron translational factors are included in each basis function to account for the fact that the electron is moving with *A*(*B*), which has a velocity \mathbf{v}_A (\mathbf{v}_B) with respect to the origin of the coordinate system.

In either the AO or MO expansion method there is no standard procedure to incorporate basis functions to represent the ionisation events. In actual numerical applications, pseudostates have been used. These are positive energy states whose wave functions have finite range. The sum of the modulus squared of amplitudes associated with these pseudostates gives the total probability for ionisation. Other methods make use of discretisation techniques that provide L^2 integrable representations of continuum states with the proper delta function normalisation for any desired value of energy. In the latter case, the differential (in energy) ionisation probability can also be computed. The latter technique has been successfully used in the case of single centre AO expansions, i.e., when all AO states are centred either in *A* or *B*. In general, single-centre expansions are adequate at high collision energies. The use of discretisation techniques in this context has been discussed in Martín and Salin (1995).

In recent years elaborate close-coupling calculations based on either AO or MO basis functions have been shown to be capable of predicting reliable excitation and charge transfer cross sections, as well as ionisation cross sections, in a broad range of energies, if the collision system can be described by a reasonable-size basis function. As an example, in Fig. 3 the total charge transfer cross sections for $C^{3+} + H$ collisions obtained by close-coupling calculations based on the atomic and molecular orbitals are shown to compare well with the experimental results from different groups (Tseng and Lin, 1999). Many other similar collision systems have been investigated in the

past two decades and more examples can be found in monographs (Bransden and McDowell, 1992) and in review articles (Fritsch and Lin, 1991; Kimura and Lane, 1990).

Figure 3 Comparison of experimental total electron capture cross sections with results from close-coupling calculations for the $C^{3+} + H$ system. Solid line is from using AO basis set, and the two dashed lines are from using MO basis set. See Tseng and Lin, (1999).



The multichannel close-coupling method, despite its well-known success, cannot be easily applied to collisions involving atoms initially prepared in Rydberg states, or for collisions when many Rydberg states are populated. In these cases the number of states needed to be included in the calculation is too large to be handled in the coupled-channel methods. The only theoretical approach available for such systems is the classical trajectory Monte Carlo method, which treats the motion of the electron classically.

Hidden Crossing Theory In recent years a new approach for ion-atom collisions at low energies, called hidden crossing theory (Solov'ev, 1990), has been proposed. It is best illustrated first for the avoided crossing of two adiabatic potentials. Starting with a diabatic Hamiltonian as in Eq. (27) where all the matrix elements are real quantities, the energy eigenvalues of this Hamiltonian is given by

$$E_{1,2}(R) = \frac{H_{11} + H_{22}}{2} \pm \frac{1}{2} \sqrt{(H_{11} - H_{22})^2 + 4H_{12}^2}, \quad (36)$$

where E_1 and E_2 are the adiabatic potentials. According to the noncrossing rule of Neumann and Wigner, these two adiabatic curves do not cross in the real- R axis, where R is the internuclear distance. However, these two adiabatic curves do cross if R is allowed to take complex values. In fact, they cross at a complex R_c satisfying

$$H_{11}(R_c) - H_{22}(R_c) = \pm 2iH_{12}(R_c). \quad (37)$$

For the Landau-Zener model the complex energy difference becomes

$$E_1(R) - E_2(R) \propto \sqrt{R - R_c}. \quad (38)$$

This equation shows that R_c is a branch point. Thus instead of two adiabatic potential curves in the real-

R axis, in the complex- R plane the potential surface is a single surface with two sheets joined at the branch point. The transition matrix element has a pole and the transition probability can be derived using Cauchy's theorem by performing contour integration on the complex- R plane. The transition probability between the two levels is

$$P_{12} = \exp\left(-\frac{2}{v}\Delta_{12}\right), \quad (39)$$

where

$$\Delta_{12} = \left| \text{Im} \int_{R_c}^{R_c} \frac{[E_1(R) - E_2(R)]}{(v_R/v)} \right| \quad (40)$$

with v_R being the radial velocity and v is the collision velocity.

This simple two-channel model can be extended to multichannel problems and used to obtain ionisation cross sections at low energies. Thus for the basic $H^+ + H$ collisions, the potential surfaces for the H_2^+ ion are calculated to search for the branch points. Two classes of branch points have been identified. The first class belongs to the so-called S promotion, which is a series of branch points located at essentially the same small real values of R . Promotion through this series of branch points is identified as prompt ionisation occurring when the two nuclei are close to each other. There is another class belonging to the T promotion where the branch points occur at increasingly larger real- R values. Promotion to the continuum along this T series is identified with electrons straddling near the top of the potential saddle from the two nuclei. As the two nuclei separate, the top of the saddle is raised and the electrons are ejected into the continuum. This is the saddle point mechanism for ionisation at low energies, analogous to the Wannier theory for electron impact ionisation of atoms at threshold energies. In calculating the probability for ionisation via each mechanism, it is taken as the product of the probabilities of Eq. (39) for each branch point encountered.

The hidden crossing theory provides a simple intuitive description of the mechanism of ionisation for ion-atom collisions at low energies. At present the phase information has not been included and the theory for treating differential cross sections is not complete yet.

Direct Integration of the Time-Dependent Schrödinger Equation

With the advent of powerful vector and parallel computers that are becoming increasingly available, another approach for ion-atom collisions is the direct numerical integration of the time-dependent Schrödinger equation on lattice grid points. Due to the long-range nature of the Coulomb force, however, a full 3D lattice solution has been made possible only

very recently (Wells *et al.*, 1996).

The formal solution of the time-dependent Schrödinger equation for small time intervals ($\Delta t = t - t_0$) is given by

$$\psi(t) = U(t, t_0)\psi(t_0). \quad (41)$$

A number of different approximations may be employed for the time-evolution operator $U(t, t_0)$

$$U(t, t_0) = \exp\{-iH\Delta t\}, \quad (42)$$

where $H = H[(t + t_0)/2]$. If the lattice grids are given in Cartesian coordinates, then at each time point, the spatial wave function is represented by its values at the discretised $N = N_x N_y N_z$ lattice points, where N_j is the number of points in coordinate j . When the wave function is represented in the configuration space, the potential energy operator is diagonal and the Cartesian kinetic energy operator is represented by a simple matrix. All algorithms used are iterative in nature and based on matrix multiplications. The lattice methods that have been used include the finite-difference representation, the Fourier collocation method and others.

As a common practice in the lattice-based method, the time-dependent wave function is often calculated inside a box of finite size where errors are introduced. For example, an *ad hoc* absorbing potential $-iW(x, y, z)$ is often employed to remove flux reflections from the boundaries. Ideally one would like to make the box as large as possible and the spacing between the grids as small as possible, but memory constraints limit a typical 3D calculation to a grid size of about $125 \times 125 \times 125$ for calculations carried out on present massive parallel computers.

The lattice-based methods in principle can be applied to ion-atom collisions at any energies. In reality, its applications so far have been limited to simple situations. It is more conveniently applied to excitation processes or target ionisation since the electron clouds for these processes are localised near the target. Electron capture to the low-lying bound states can be calculated so long as the electron cloud for these states does not lie near the box edge. While total ionisation cross sections can be estimated from the flux loss, information on the ejected electron momentum distributions is not available. In comparison with the close-coupling methods, the lattice-based methods do not provide advantages so far. The best results from both approaches are quite comparable but the lattice-based methods in general take many more computing resources.

The time-dependent Schrödinger equation can be solved directly also in momentum space (Sidky and Lin, 1998). For ion-atom collisions, the solution in momentum space appears to offer some advantages. Unlike the coordinate-space wave function, which ex-

tends over a large volume when the two nuclei are well separated at the end of the collision, the momentum-space wave function remains finite throughout the collision. In fact the two nuclei are fixed in the momentum space and since high-momentum components of the wave function are small, reflections from the wall in the momentum space are negligible. While it is possible to use grid-based methods to calculate the momentum-space wave function, computationally it is less taxing to employ the two-centre expansion in the momentum space. The angular parts of the basis functions are spherical harmonics and the radial momentum functions are expanded at lattice grid points. Since the integral equations in momentum space are difficult to calculate, the time integration is performed in the coordinate space. By using a least-squared fitting procedure and Runge-Kutta fixed time-step integration, such calculations can be carried out on personal computers instead of on shared supercomputers. By projecting out the bound states on each centre, excitation and charge transfer probabilities can be extracted as in the close-coupling methods. Using this approach the momentum distributions of the ejected electrons can also be obtained directly. This method offers a direct non-perturbative approach for calculating the momentum distributions of the ionisation cross sections in ion-atom collisions.

Perturbation Approaches

For collisions at higher energies perturbative approaches may be used to obtain the scattering cross sections. Consider the Hamiltonian of one electron in the field of a target of charge Z_T and projectile of charge Z_P again. Take the position vector of the electron with respect to the target and the projectile to be \mathbf{x} and \mathbf{s} , respectively. One can write the Hamiltonian in the “prior” (i) and the “post” (f) form,

$$H_{el} = H_i + V_i = H_f + V_f \quad (43)$$

and introduce the unperturbed initial and final state wave functions

$$\begin{aligned} \left(H_i - i\frac{\partial}{\partial t}\right)\Phi_i^{\text{FBA}}(\mathbf{r}, t) &= 0 \\ \left(H_f - i\frac{\partial}{\partial t}\right)\Phi_f^{\text{FBA}}(\mathbf{r}, t) &= 0. \end{aligned} \quad (44)$$

For ionisation, which is the dominant process at high energies,

$$\begin{aligned} H_i = H_f &= -\frac{1}{2}\nabla_r^2 - Z_T/x \\ V_i = V_f &= -Z_P/s \end{aligned} \quad (45)$$

and the initial and final state wave functions of (45) are given by the hydrogenic ground state and continuum Coulomb functions, respectively, multiplied by the plane-wave phase factor. The first-order per-

turbation theory for the ionisation amplitude is then given by

$$\mathcal{A}_{ik}^{\text{FBA}}(\mathbf{b}) = -i \int_{-\infty}^{+\infty} dt \left\langle \Phi_k^{\text{FBA}} \left| \frac{-Z_P}{s} \right| \Phi_i^{\text{FBA}} \right\rangle, \quad (46)$$

for each impact parameter \mathbf{b} . This formulation is valid for direct ionisation where the continuum electron sees the Coulomb field of the target ion. The expression (46) is the semiclassical version of the first Born approximation. Clearly the cross section scales with Z_P^2 within the first Born approximation.

The first Born approximation neglects the influence of the Coulomb field from the projectile charge on the initial and final state wave functions. While such influence can be partially accounted for by calculating the higher order terms of the Born series, these higher Born amplitudes are difficult to evaluate. Instead it is preferable to introduce distorted wave models where such influence can be included partially in the first-order theory.

For this purpose, one rewrites the Hamiltonian formally as

$$\begin{aligned} H_{\text{el}} &= H_i + V_i = H_i + U_i + W_i = H_i^{\text{d}} + W_i \\ H_{\text{el}} &= H_f + V_f = H_f + U_f + W_f = H_f^{\text{d}} + W_f \end{aligned} \quad (47)$$

to introduce the distortion potentials U_i and U_f for the initial state and the final state, with W_i and W_f the residual interactions, respectively. The distortion potentials are chosen such that the Schrödinger equations

$$\begin{aligned} \left(H_i^{\text{d}} - i \frac{\partial}{\partial t} \right) \chi_i^+(r, t) &= 0 \\ \left(H_f^{\text{d}} - i \frac{\partial}{\partial t} \right) \chi_f^-(r, t) &= 0 \end{aligned} \quad (48)$$

have solutions of the form

$$\chi_i^+(r, t) = \Phi_i^{\text{FBA}}(r, t) \mathcal{L}_i^+(r) \quad (49)$$

$$\chi_f^-(r, t) = \Phi_f^{\text{FBA}}(r, t) \mathcal{L}_f^-(r). \quad (50)$$

This imposes on the distortion term the condition

$$\begin{aligned} \Phi_i^{\text{FBA}} \left(-\frac{1}{2} \nabla_s^2 - \frac{Z_P}{s} + i\mathbf{v} \cdot \nabla_s \right) \mathcal{L}_i^+ \\ = \Phi_i^{\text{FBA}} (\nabla_x \ln \phi_i(x) \cdot \nabla_s \mathcal{L}_i^+). \end{aligned} \quad (51)$$

If the right-hand side of (51) is neglected, then the above equation can be solved analytically to obtain

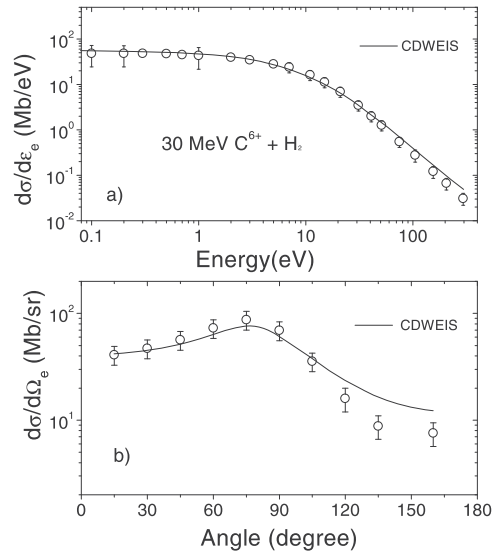
$$\mathcal{L}_i^{\text{CDW}}(r) = N(\nu) {}_1F_1(i\nu; 1; i\nu s + i\mathbf{v} \cdot \mathbf{s}), \quad (52)$$

where $N(a) = \exp(\pi a/2) \Gamma(1 - ia)$, $\nu = Z_P/|\mathbf{k} - \mathbf{v}|$ and ${}_1F_1$ is the confluent hypergeometric function; i.e., (52) is a Coulomb function of momentum $\mathbf{k} - \mathbf{v}$ with respect to the projectile centre. This approximation is called the continuous distorted wave (CDW) approximation. If the Laplacian in (51) is also neglected, then

$$\mathcal{L}_i^{\text{EIS}}(r) = \exp(-i\mathbf{v} \ln(\nu s + \mathbf{v} \cdot \mathbf{s})) \quad (53)$$

and the resulting approximation is called the eikonal initial state (EIS) distortion. By using the CDW wave function for the final state and the EIS wave function for the initial state, the so-called CDW-EIS theory has been widely used to calculate the ionisation cross sections, both integral and differential, for a wide range of collision systems. In the intermediate- to high-energy region, such calculations have been found to work well, accounting for most of the two-centre effects that are not present in the first Born approximation. In Fig. 4 the ionisation of H_2 molecules by 30-MeV C^{6+} ions is used to illustrate that the CDW-EIS theory is capable of predicting the details of the differential cross sections for such systems (Tribedi *et al.*, 1996). More details of ionisation processes can be found in the monograph by Stolterfoht *et al.* (1997).

Figure 4 Single differential cross sections for ionisation for $\text{C}^{6+} + \text{H}_2$ collisions at 30 MeV and comparison to the predictions from the first Born approximation and from the CDW-EIS theory. Adopted from Tribedi *et al.* (1996).



Relativistic Ion-Atom Collisions

Relativistic atomic collisions involving highly charged ions with charge number up to $Z=92$ and energies ranging from 100 MeV/amu upwards constitute a new field where the quantum electrodynamics (QED) vacuum plays a role. For relativistic collisions, in addition to the well-known atomic processes such as excitation, electron capture and ionisation, the intense electromagnetic fields make the creation of free electron-positron pairs and other processes from the QED vacuum possible. The nonradiative electron capture process, which is the dominant mechanism for electron capture at lower energies, becomes less important at high energies than the radiative elec-

tron capture process. At still higher energies, electron capture from the pair production (CPP), which does not exist at lower energies, becomes the dominant electron capture processes at extreme relativistic energies. The CPP process was first observed experimentally in 1992. It is a bound-free pair production where the electron–positron pair is created from the vacuum with the end result that the electron is captured to the bound states of the incident ion and a free positron is ejected into the continuum. For high- Z target atoms, CPP cross section has been observed to increase with increasing relativistic energies, in contrast to the rapid decrease with increasing energies for the electron capture processes. Note that CPP can proceed between two bare ions colliding at relativistic energies with the end results that the ion charge state decreases by one unit. This mechanism has been predicted to account for more than half of the beam loss for bare ions in the Relativistic Heavy Ion Collider (RHIC) at Brookhaven, and for the bare ions in the Large Hadron Collider (LHC) at CERN. Interestingly, this mechanism is also responsible for the production of antihydrogen when antiprotons are bombarded on Xe targets at the relativistic momentum of 2–6 GeV/ c .

Consider the collision between a fully stripped projectile ion with charge Z_P on a one-electron ion with charge Z_T , in the impact parameter approximation where the projectile is travelling along a straight-line trajectory with impact parameter \mathbf{b} and velocity \mathbf{v} , the relativistic Dirac Hamiltonian is

$$H_D = H_0 + V_P(t), \quad (54)$$

where H_0 is the target Hamiltonian

$$H_0 = -i\alpha \cdot \nabla + \beta - Z_T e^2/r, \quad (55)$$

with α and β being the Dirac matrices, and V_P is the time-dependent perturbation by the projectile

$$V_P(\mathbf{r}') = -Z_P \alpha \gamma (1 - v\alpha_z)/r', \quad (56)$$

where $r' = \sqrt{(x-b)^2 + y^2 + \gamma^2(z-vt)^2}$, α is the fine structure constant and γ is the Lorentz factor. This expression is derived from the Lienard–Wiechert potential of a moving charge. In relativistic theories, natural units are often used ($\hbar = m = c = 1$) as in the two equations above. According to the intuitive Dirac hole theory, the initial state can be considered as given by an electron in the K shell, together with a fully occupied negative continuum. For describing pair production, on the other hand, the initial state is a fully occupied negative continuum only. For the latter, the presence of the K -shell electron does not enter. This simple intuitive picture is valid if the electron–electron two-body interaction can be neglected and the time evolution of each electron is independent. This independent particle picture allows the reduction of the

many-particle amplitudes in terms of single-particle amplitudes, and the calculation can be carried out in the framework of the Dirac Hamiltonian, Eq. (54).

The simplest theoretical method for solving the time-dependent Dirac equation is to use the lowest order perturbation theory. The transition amplitude from an initial state i to a final state f is given by

$$A_{fi}(\mathbf{b}) = i\gamma Z_P \alpha \int_{-\infty}^{\infty} dt e^{i(E_f - E_i)t} \times \int d^3r \psi_f^\dagger(\mathbf{r}) \frac{1 - v\alpha_z}{r'} \psi_i(\mathbf{r}). \quad (57)$$

Clearly this expression can be used to evaluate the excitation or the direct ionisation of the electron from the K shell, for example, and it would give the Z_P^2 dependence of the cross sections. Using the analogy to the ionisation process, Eq. (57) can also be used to evaluate pair production cross sections by a charged particle. The complication lies in the actual calculation since both the initial and final states are continuum states. A perturbative approach for the CPP can be obtained by treating it as an electron being transferred from a negative-energy state in the target field to a bound state of the projectile. By employing the first-order theory the charge transfer amplitude is

$$A_{fi}(\mathbf{b}) = iZ_T \alpha \int_{-\infty}^{\infty} dt \int d^3r \psi_f^\dagger(\mathbf{r}') \hat{S}^{-1} \times \frac{1}{r} \psi_i(\mathbf{r}) e^{i(E_i t' - E_f t)}, \quad (58)$$

where S is a Lorentz boost operator (see Eq. 4.29 of Eichler and Meyerhof (1995)) to transform the final-state wave function from the projectile to the target system.

For relativistic collisions by multiply charged ions, nonperturbative methods for solving the time-dependent Dirac equation are needed. As in the nonrelativistic case, close-coupling methods using the equivalent of atomic or molecular orbitals have been used. Direct numerical solutions in the coordinate space or in the momentum space by expanding the wave functions in lattice points have also been used. Details can be found in the book by Eichler and Meyerhof (1995).

§4. Atomic Collisions with Multielectron Targets

The previous two sections describe the basic scattering theories that have been widely used for treating the different inelastic processes in atomic collisions over a broad range of collision energies. The theories have been presented for the prototype systems consisting of one electron and two heavy particles. Most of the methods can be formally generalised in a straightforward manner for many-electron targets of atoms, molecules, clusters and surfaces. However, in actual applications for such collisions many more approxi-

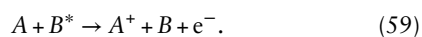
mations must be implemented since representing the time-dependent wave function of a many-electron system over the whole collision time in terms of basis functions or on lattice grids is essentially impossible.

There are two situations where approximate calculations on many-electron systems can be made using *ab initio* scattering theories. For low-energy collisions, if the number of inelastic channels excited is limited, then it is possible to use many-electron molecular or atomic wave functions as basis set in a close-coupling expansion of the time-dependent wave function.

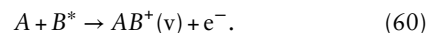
For collisions at higher energies, multielectron processes can occur in addition to the single-electron processes. For single ionisation, single-electron capture or single-excitation processes, it is often possible to employ the active electron model, with the other electrons that are not involved in the processes treated as passive electrons. In such models the multielectron system is reduced to a single-electron system with the active electron being in the screened field of the target and projectile ions. For multielectron processes, for example, double ionisation or electron capture accompanied by ionisation, full *ab initio* calculations are difficult to perform. Thus the independent-electron models are often used. In this model, the many-electron wave function is written as the antisymmetrised product of the wave functions of individual electrons, so that electron correlation is neglected. In such models amplitudes for multielectron processes can be written as antisymmetrised products of single-electron amplitudes. Such independent-electron models have been used to describe multielectron processes in ion-atom collisions with some success. However, there are many circumstances where such simple models fail. A few examples of such calculations can be found in Fritsch and Lin (1991). A step forward in including electron correlation in the dynamics of fast collision processes is provided by the *frozen correlation approximation* (FCA) (Martín and Salin, 1996). In this method, electron correlation is included in both the initial and final states but it is frozen during the collision. In this way, a many-electron transition amplitude can be written as a linear combination of antisymmetrised products of one-electron amplitudes.

§5. Penning Ionisation and Associative Ionisation

Penning ionisation (PI) is the process in which an energy donor B^* collides with a neutral atom or molecule A whose ionisation energy is less than the excitation contained in B^* , A loses one of its electrons and B remains in the ground state. It can be represented by the reaction



This process was first suggested by Frans Penning in 1927. Besides PI, another process is associative ionisation (AI) represented by



PI and AI are only effective at thermal energies. Therefore, the collision velocities are much smaller than the typical electron velocities, which suggests the use of a quasimolecular picture in the framework of the Born–Oppenheimer (BO) approximation. The basic mechanism responsible for PI and AI is that of a bound molecular state (correlated with the entrance channel $A + B^*$) that is embedded in a molecular electronic continuum (correlated with the exit channel $A + B^+ + e^-$) to which the former state is coupled by the electron–electron interaction (see Fig. 5). Thus, PI and AI can be interpreted as resonant processes similar to those observed in atomic and molecular photoionisation.

Excellent surveys of the different experimental and theoretical techniques used to study reactions (59) and (60) have been published by Siska (1993) and Weiner *et al.* (1990), respectively. The theory of PI and AI involves both electronic structure aspects and collision dynamics aspects. The former include evaluation of correlated molecular states and the coupling with the molecular electronic continuum. In this section only the basic formalism that connects structural and dynamical aspects will be discussed. Since PI dominates AI at thermal energies (see below), in a first step one can assume that the total ionisation cross section results from reaction (59) almost exclusively. Then one can treat the problem semiclassically in this sense: the nuclei follow classical trajectories in the field induced by the effective interatomic potential, whereas the electrons are described quantum mechanically. Thus, on any given nuclear trajectory, the electronic wave function is the solution of a time-dependent Schrödinger equation as that of Eq. (24).

Resonant processes are conveniently described in terms of a projection operator formalism. With the picture provided by Fig. 5 in mind, we define a basis of adiabatic states as follows. Bound electronic states AB^* lying above the ionisation threshold AB^+ are formally the solutions of

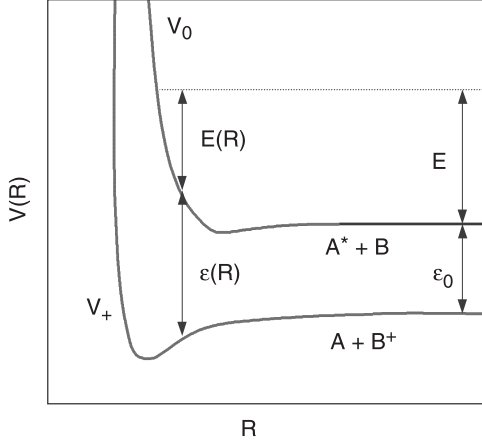
$$(QH_{\text{el}}Q - E_i)\psi_i = 0 \quad (61)$$

and unbound ($AB^+ + e^-$) electronic continuum states are the solution of

$$(P_l H_{\text{el}} P_l - E)\Psi_{E,l} = 0, \quad (62)$$

where l is the angular momentum of the ejected electron, and P_l and Q are projection operators that satisfy the conditions $P_l P_{l'} = \delta_{ll'}$, $P = \sum_l P_l$, $PQ = 0$ and $P + Q = 1$ for all R . Notice that H_{el} is not diagonal in the $\{\psi_i, \Psi_{E,l}\}$ basis because, in general,

Figure 5 Two-potential energy curve model for Penning ionisation. E is the centre-of-mass kinetic energy of collision, ϵ_0 is the separation of the reagent and product potential asymptotes, $E(R)$ is the (classical) local heavy-particle kinetic energy and $\epsilon(R)$ is the kinetic energy of the Penning electron when PI occurs at separation R .



$\langle \psi_i | \mathcal{Q} \mathcal{H}_{el} P_I | \psi_{E,l} \rangle$ and $\langle \psi_{E,l} | P_I \mathcal{H}_{el} P_I | \psi_{E,l} \rangle$ are different from 0. Therefore, the $\{\psi_i, \psi_{E,l}\}$ basis is adiabatic in the sense that Eqs. (61) and (62) are fulfilled for all R . The electronic wavefunction $\Psi(t)$ is expanded in this basis

$$\Psi(t) = \sum_i c_i(t) \psi_i \exp\left(-i \int_{-\infty}^t E_i dt'\right) + \sum_l \int dE_{E,l}(t) \psi_{E,l} \exp\left(-i \int_{-\infty}^t E dt'\right), \quad (63)$$

where ψ_0 represents the initial state. The initial condition is $c_i(-\infty) = \delta_{i0}$, $c_{E,l}(-\infty) = 0$. Substitution of Eq. (63) in the Schrödinger equation leads to the system of differential equations

$$i \frac{d}{dt} c_i(t) = \sum_l \int dE \exp\left(i \int_{-\infty}^t (E_i - E) dt'\right) \langle \psi_i | \mathcal{Q} \mathcal{H}_{el} P_I | \psi_{E,l} \rangle c_{E,l}(t) \quad (64)$$

$$i \frac{d}{dt} c_{E,l}(t) = \sum_i c_i(t) \exp\left(i \int_{-\infty}^t (E - E_i) dt'\right) \langle \psi_{E,l} | P_I \mathcal{H}_{el} \mathcal{Q} | \psi_i \rangle + \sum_{l' \neq l} \int dE' c_{E',l'}(t) \times \exp\left(i \int_{-\infty}^t (E - E') dt'\right) \langle \psi_{E,l} | P_I \mathcal{H}_{el} P_I | \psi_{E',l'} \rangle. \quad (65)$$

In the latter equations, all dynamical couplings corresponding to breakdown of the BO approximation have been neglected. This is a very good approximation because the dynamical couplings are proportional to the collision velocity which, in the case of PI, is on the order of 10^{-3} au. The couplings $\langle \psi_i | \mathcal{Q} \mathcal{H}_{el} P_I | \psi_{E,l} \rangle$ are responsible for bound-continuum transitions while the $\langle \psi_{E,l} | P_I \mathcal{H}_{el} P_I | \psi_{E,l} \rangle$ couplings represent continuum-continuum transitions and, therefore, they are responsible for a redis-

tribution of the population within the continuum. As usual, the total ionisation cross section is given by integrating the probability

$$P(b) = \lim_{t \rightarrow \infty} \sum_l \int dE |c_{E,l}(t)|^2 \quad (66)$$

over the impact parameter plane, where b is the impact parameter.

In most applications, instead of solving the system of coupled equations (64) and (65), one makes use of a local approximation. This approximation can be easily derived from (64) and (65) by assuming that (i) the entrance channel is well separated in energy from the remaining \mathcal{Q} states (isolated resonance approximation) and (ii) all continuum-continuum couplings within P subspace are 0. Using approximations (i) and (ii) in Eq. (65), integrating over time and substituting the result into Eq. (64), one obtains

$$\frac{d}{dt} c_0(t) = - \sum_l \int dE | \langle \psi_0 | \mathcal{Q} \mathcal{H}_{el} P_I | \psi_{E,l} \rangle |^2 \times \int_{-\infty}^t dt' c_0(t') \exp\left(i \int_{t'}^t (E_0 - E) dt''\right). \quad (67)$$

Let ΔE be the energy interval such that $\langle \psi_0 | \mathcal{Q} \mathcal{H}_{el} P_I | \psi_{E,l} \rangle$ barely changes in the interval $I_{E_0} = [E_0 - \Delta E, E_0 + \Delta E]$. If the collision velocity $\mathbf{v}(t) = \mathbf{v}_0 - \mu^{-1} \int_{-\infty}^t \nabla V dt'$ (where V is the interatomic potential, μ the reduced mass of the nuclei and \mathbf{v}_0 the initial velocity) is small enough such that $|\mathbf{v}| < \Delta E$ for all t , the integral in Eq. (67) is almost 0 outside I_{E_0} due to the strongly oscillatory behaviour of the exponential. Then Eq. (67) can be easily integrated and the total ionisation probability for a given trajectory can be written

$$P(b) = 1 - \exp\left(- \int_{-\infty}^{\infty} \Gamma(t) dt\right), \quad (68)$$

where

$$\Gamma(t) = 2\pi \sum_l | \langle \psi_0 | \mathcal{Q} \mathcal{H}_{el} P_I | \psi_{E=E_0,l} \rangle |^2. \quad (69)$$

Equation (68) can also be written as

$$P(b) = 1 - \exp\left(-2 \int_{R_0}^{\infty} \frac{\Gamma(R)}{v_b(R)} dR\right), \quad (70)$$

where $v_b(R)$ is the radial velocity of the nuclei. In general, the value of the width $\Gamma(R)$ decreases exponentially with R and, therefore, the ionisation probability is only important at short internuclear distances. Similar results have been obtained from purely classical considerations (Miller, 1970). In many experimental and theoretical studies, the energy donor is a noble-gas metastable atom. Figure 6 shows the energy dependence of the Penning ionisation cross section in the case of the $\text{Ne}^*(^3P_2) + \text{H}$ collision. It can be seen that the cross sections decreases monotonically with impact energy, which is the typical behaviour in most cases. To find the probability distribution $P(b, \epsilon)$, so that $P(b, \epsilon) d\epsilon$ is the probability that the energy of the ejected electron lies in the interval

($\epsilon, \epsilon + d\epsilon$), one notes that the transition occurs at internuclear distance R , then the energy of the ejected electron must be $\epsilon(R) = V(R) - V_+(R)$, where $V_+(R)$ is the potential energy curve of the residual molecular ion AB^+ . The probabilities $P(b, \epsilon)$ and $P(R)$ are related by $P(b, \epsilon)d\epsilon = P(R)dR$ so that

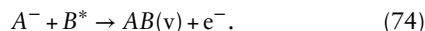
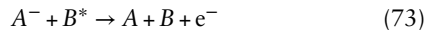
$$P(b, \epsilon) = \sum_i P(R_i) / |d\epsilon/dR|_{R_i}, \quad (71)$$

where the sum is over those R_i (usually no more than 2) that satisfy $\epsilon = V(R_i) - V_+(R_i)$.

AI can arise only if the potential of the AB^+ ion, $V_+(R)$, possesses a well deep enough to support bound vibrational states. If the energy carried away by the ionised electron is $\epsilon = V(R) - V_+(R)$ then the relative translational energy is $E - \epsilon$, where E is the kinetic energy $E = \mu v_0^2/2$ of the collision. Hence, $E - \epsilon < 0$ implies that the final relative motion in the V_+ potential must be that of a bound state of AB^+ , that is, AI. The probability for AI is then given by (Siska, 1993)

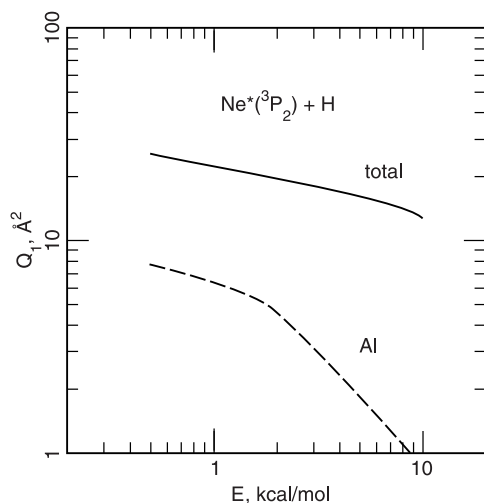
$$P_{\text{AI}}(b) = 2 \exp \left(- \int_{R_0}^{\infty} \frac{\Gamma(R)}{v_b(R)} dR \right) \sinh \left(\int_{R_0}^{R_{\text{AI}}} \frac{\Gamma(R)}{v_b(R)} dR \right), \quad (72)$$

where R_{AI} is the (unique) root of $E - \epsilon(R) = 0$. A similar theoretical framework has been recently proposed (Martín and Berry, 1997) to study electron detachment from negative ions using excited neutrals:



The processes are called, respectively, Penning detachment (PD) and associative detachment (AD). PD cross sections are several orders of magnitude larger than PI cross sections. The explanation is twofold and is

Figure 6 Theoretical prediction of total and AI cross sections for $\text{Ne}^+ + \text{H}$. As mentioned in the text, the total ionisation cross section is close to the PI cross section. Taken from Siska (1993).



related to the presence of a negative charge in the projectile. In the first place, Stark mixing between excited states of B^* is induced by the charged projectile A^- . As a result of this mixing, the width $\Gamma(R)$, which represents the coupling between the entrance channel and the continuum, does not decrease exponentially, but rather $\Gamma \sim R^{-6}$, which is typical of dipole-dipole interactions. In the second place, the interatomic potential $V(R)$ between a negative ion and a neutral is given by $-\alpha/R^4$, where α is the polarisability, and may be more attractive than between two neutrals. This attractive potential may also lead to orbiting of the projectile around the target.

§6. Ion-Molecule Collisions

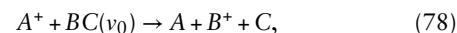
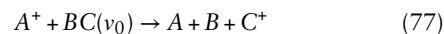
In this section electronic and vibrational transitions in ion-molecule collisions are considered. The reactive scattering is being addressed separately in Chapter 2.6.4. Only collisions between ions and diatomic molecules will be considered, including processes like charge transfer



electronic and/or vibrational excitation



and dissociative charge transfer



in the impact energy range from a few millielectronvolts to several kiloelectronvolts. The first significant attempts to investigate this problem were based on a classical treatment of all nuclear degrees of freedom and a quantum mechanical treatment of the electronic motion (see, e.g., the review of Kleyn *et al.* (1982) and the book by Bernstein (1979)). More recently, fully quantum mechanical and semiclassical methods have become available. These methods have been extensively reviewed by Sidis (1990). In this section, the most common approximations are discussed.

Although not discussed in detail in this chapter, we should mention another important area of research, namely that of rotational excitation without any vibrational or electronic transition. Studies on this topic began in the early 1970s (see, e.g., Pack (1974) and references therein) and opened up the way to various approximations, such as the infinite order sudden approximation discussed below, which is widely used in present computations of vibronic excitations in ion-molecule collisions.

Quantum Mechanical Approach

After removal of the centre-of-mass motion and neglecting the small mass polarisation terms, the non

relativistic Hamiltonian of the $A + BC$ system can be written

$$\mathcal{H} = -\frac{1}{2\mu}\nabla_{\mathbf{R}}^2 - \frac{1}{2m}\nabla_{\rho}^2 - \frac{1}{2}\sum_{i=1}^N\nabla_{\mathbf{r}_i}^2 + V(\mathbf{r}, \mathbf{R}, \rho, \gamma), \quad (79)$$

where the set of electronic coordinates \mathbf{r}_i is called \mathbf{r} , N is the number of electrons, $\rho = BC$ (see Fig. 7), $\mathbf{R} = OA$, O is the centre of mass of nuclei B and C , and the masses μ and M are given by $\mu = m_A(m_B + m_C)/(m_A + m_B + m_C)$, $m = m_B m_C/(m_B + m_C)$. In general, the electronic motion is described in the so-called body-fixed (BF) reference frame that accompanies the overall rotation of the three nuclei about the nuclear centre of mass. In contrast, the nuclear motion is usually treated in the laboratory reference frame. In the quantum mechanical approach, one solves the Schrödinger equation

$$\mathcal{H}\Psi(\mathbf{r}, \mathbf{R}, \rho) = E\Psi(\mathbf{r}, \mathbf{R}, \rho) \quad (80)$$

by expanding the wave functions in a basis of adiabatic states Φ_n

$$\Psi(\mathbf{r}, \mathbf{R}, \rho) = \sum_n C_n(\mathbf{R}, \rho)\Phi_n(\mathbf{r}, \mathbf{R}, \rho, \gamma). \quad (81)$$

The Φ_n states are eigenfunctions of the electronic Hamiltonian

$$\mathcal{H}_{\text{el}} = -\frac{1}{2}\sum_{i=1}^N\nabla_{\mathbf{r}_i}^2 + V(\mathbf{r}, \mathbf{R}, \rho, \gamma), \quad (82)$$

so that

$$\mathcal{H}_{\text{el}}\Phi_n(\mathbf{r}, \mathbf{R}, \rho, \gamma) = E_n\Phi_n(\mathbf{r}, \mathbf{R}, \rho, \gamma). \quad (83)$$

This is similar to the molecular method in ion-atom collisions (see Molecular Orbital Expansion Method). The nuclear wave function can be expanded

$$C_n(\mathbf{R}, \rho) = \sum_{\nu} F_{\nu\nu}(\mathbf{R})G_{\nu\nu}(\rho), \quad (84)$$

where $G_{\nu\nu}$ is usually written as a product of a vibrational function $\chi_{\nu\nu}$ and a rotational wave function $Y_{j_n m_n}$ of the isolated BC molecule

$$G_{\nu\nu}(\rho) = \frac{\chi_{\nu\nu}(\rho)}{\rho} Y_{j_n m_n}(\hat{\rho}). \quad (85)$$

The wave functions $\Phi_n(\mathbf{r}, \mathbf{R}, \rho, \gamma)$ and $G_{\nu\nu}(\rho)$ form complete orthogonal basis sets for the variables \mathbf{r} and ρ . Substituting expansions (81) and (84) into the Schrödinger equation (80), and projecting into the $G_{\nu\nu}\Phi_n$ basis leads to the system of coupled equations

$$\begin{aligned} & \langle G_{\nu\nu}\Phi_n | \mathcal{H} - E | G_{\nu'\nu'}\Phi_{n'} \rangle F_{\nu'\nu'}(\mathbf{R}) \\ & = - \sum_{n'\nu'} \langle G_{\nu\nu}\Phi_n | \mathcal{H} | G_{n'\nu'}\Phi_{n'} \rangle F_{n'\nu'}(\mathbf{R}). \end{aligned} \quad (86)$$

Solutions of (86) yields for $R \rightarrow \infty$ the scattering amplitudes that determine the state-to-state cross sections. Even with the nonadiabatic couplings at hand, evaluation of the transition amplitudes using this general formalism is a formidable task due to the large number of terms contained in Eq. (86). Indeed, to solve Eq. (86), one usually writes the nuclear wave

functions $F_{\nu\nu}$ as a partial wave expansion

$$F_{\nu\nu}(\mathbf{R}) = \sum_{lm} \frac{F_{\nu\nu}^l(\mathbf{R})}{R} Y_{lm}(\theta, \phi), \quad (87)$$

where the Y_{lm} spherical harmonics depend on the polar angles associated with the \mathbf{R} vector (see Fig. 7). A way out of this problem appears when (i) the collision time is small compared to the rotational period of the BC molecule and (ii) the radial relative motion is faster than the angular relative motion. In this case the orientations of both the BC molecule and the \mathbf{R} vector can be considered as fixed in space. Assumptions (i) and (ii) are called, respectively, the *energy-sudden approximation* and the *centrifugal-sudden approximation*. Both approximations are the basis of the infinite order sudden (IOS) approximation, which consists in replacing all coupled values of j and l by common values \bar{j} and \bar{l} compatible with the value of the total angular momentum. As a consequence, the resulting system of coupled equations is partially diagonalised, thus leading to a more tractable problem.

Semiclassical Approach

For collisions at higher velocities, the motion of the projectile can be described classically. In this case, the Schrödinger equation one must solve is formally identical to that of Eq. (24) except that now \mathcal{H}_{el} must be replaced by the internal Hamiltonian \mathcal{H}_{int} ,

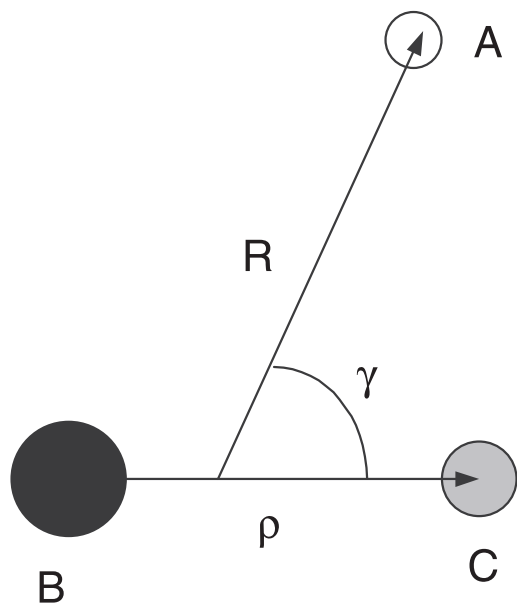
$$\mathcal{H}_{\text{int}} = \mathcal{H}_{\text{el}} - \frac{1}{2m}\nabla_{\rho}^2. \quad (88)$$

Typically, the semiclassical method is valid for collision energies above 50 eV/amu. At these collision energies, the BC rotor remains practically fixed in space during the collision, so that one can use the energy-sudden approximation. This is not the case for the centrifugal-sudden approximation, which can be very poor at high collision energies. Therefore, from the two conditions for the validity of the IOS approximation, only the first one is fulfilled. In addition, when the collision energy is on the order of 100 eV/amu, the collision time is shorter than the vibrational period of the BC molecule. Consequently, the initial vibrational wave function does not appreciably change in the time interval in which the electronic transitions take place. This is called the *vibrational-sudden approximation*. Thus, the wave function describing the collisional system can be expressed as

$$\Psi(\mathbf{r}, \rho, t) = \rho^{-1} Y_{j_n m_n}(\hat{\rho}) \chi_{\nu\nu}(\rho) \psi(\mathbf{r}, \rho, t) \quad (89)$$

with $\psi(\mathbf{r}, \rho, t)$ describing the electronic structure. In the context of the semiclassical approach, Eq. (89) is simply called the sudden approximation and should not be confused with the IOS approximation introduced in the previous section. As mentioned above, the present sudden approximation is a very good approximation in almost the entire energy range in

Figure 7 Set of internal coordinates R , ρ , γ for an $A + BC$ collisional system.



which the semiclassical treatment is valid. Furthermore, one can use the impact parameter or eikonal method in which the position vector \mathbf{R} of the incident ion with respect to the centre of the diatom is assumed to follow classical straight-line trajectories with constant velocity \mathbf{v} and impact parameter \mathbf{b} : $\mathbf{R} = \mathbf{b} + \mathbf{v}t$ (Errea *et al.*, 1997, 1999). In a close-coupling molecular approach the electronic wave function $\psi(\mathbf{r}, \rho, t)$ of (89) is expanded in terms of the set of (approximate) eigenfunctions $\{\phi_i\}$ of the Born–Oppenheimer electronic Hamiltonian, \mathcal{H}_{el} :

$$\mathcal{H}_{\text{el}} \phi_i(\mathbf{r}; \mathbf{R}, \rho) = \varepsilon_i(\mathbf{R}, \rho) \phi_i(\mathbf{r}; \mathbf{R}, \rho). \quad (90)$$

For each value of ρ , this expansion takes on the form

$$\psi(\mathbf{r}, \rho, t) = \sum_j a_j(t; \rho) \phi_j(\mathbf{r}, \rho, \mathbf{R}) \exp\left(-i \int_0^t \varepsilon_j dt'\right). \quad (91)$$

The expansion coefficients $a_j(t; \rho)$ are then obtained by substituting (89) and (91) into the time-dependent Schrödinger equation. For a given nuclear trajectory and fixed ρ , one obtains that

$$i \frac{da_j}{dt} = \sum_k a_k \langle \phi_j | \mathcal{H}_{\text{el}} - i \frac{\partial}{\partial t} \Big|_{\mathbf{r}, \rho} | \phi_k \rangle \times \exp\left(-i \int_0^t (\varepsilon_k - \varepsilon_j) dt'\right). \quad (92)$$

The a_j coefficients are subject to the initial condition $a_j(t \rightarrow -\infty; \rho) = \delta_{ij}$. The transition probability $P_{v'f}$ to the $\{v'f\}$ vibronic state is obtained by projecting the wave function (89) onto the final state, and summing over all rotational exit channels. When for a given j all values of m_j are equally probable, the sum over all initial m_j values leads to an orientation-averaged

transition probability of the form

$$P_{v'f}(\mathbf{b}, v) = (4\pi)^{-1} \int d\hat{\rho} \left| \int d\rho \chi_{v'}(\rho) \chi_v(\rho) \times \exp\left(-i \int_0^\infty dt (\varepsilon_f - E_f)\right) a_f(\infty; \rho) \right|^2. \quad (93)$$

The total cross sections are obtained by integrating the transition probabilities of Eq. (93) over the impact parameter plane. It is generally assumed that at high collision energies the population of the vibrational states of the BC molecule subsequent to electronic transitions obeys the Franck–Condon (FC) principle. The FC expression of the transition probabilities is obtained if one assumes that the coefficients $a_f(\infty; \rho)$ are slowly varying functions of ρ , and substitutes them with the values at the equilibrium distance of the BC molecule ρ_0 :

$$P_{v'f}^{\text{FC}}(\mathbf{b}, v) = \int d\hat{\rho} |a_f(\infty; \rho_0)|^2 \left[\int d\rho \chi_{v'}(\rho) \chi_v(\rho) \right]^2. \quad (94)$$

Calculations of ion–molecule cross sections involve *ab initio* electronic data, namely potential energy surfaces, which can be accurately calculated using state-of-the-art quantum chemistry programs and couplings, which constitute the real bottleneck for applications of the theory described above. An illustration of the importance of the various processes that take place in ion–molecule collisions is shown in Fig. 8 for the $\text{C}^{4+} + \text{H}_2$ collision. The dominant process is single-charge transfer. However, it can be seen that dissociative charge transfer becomes competitive with the nondissociative process at the lower impact energies. In this reaction, dissociation is due to a transition from the original vibrational state to the vibrational continuum and not to a direct transition to an electronic dissociative state. Vibrational excitation is also a very important process; in fact it is the dominant process at the lower energies. Figure 8 also shows results obtained within the FC approximation. The latter approximation is independent of the initial vibrational state of H_2 and cannot describe vibrational excitation.

§7. Ion–Cluster Collisions

In the past decade, there has been an increasing interest in the study of collisions between ions and clusters, especially metal clusters and fullerenes. The processes that can take place in this kind of collision are similar to those observed in ion–molecule collisions: they involve simultaneously electronic transitions (charge transfer, excitation, ionisation) and nuclear-core excitations (vibration, rotation, fragmentation). As the number of electronic and nuclear degrees of freedom is large, the use of fully quantum mechanical methods is not yet possible. This complexity also explains why, in contrast with important experimental progress, the

theoretical understanding of these processes is still modest. Till the mid-1990s, most theoretical studies were performed using classical mechanics with phenomenological two- or three-body potentials to describe the interatomic forces. These purely classical methods are usually called molecular dynamics (MD) methods, for which there is an extensive literature and well-documented computational packages.

Recently theoretical methods that go beyond MD by including quantum effects have begun to emerge. To date, quantum theoretical methods can be classified into two different categories. In the first, for which most applications have been developed, one makes use of the jellium approximation to describe the isolated cluster. In this approximation one replaces the real ionic distribution of the cluster with a homogeneous positively charged distribution whose role is to ensure cluster neutrality. This is a good approximation for metal clusters such as sodium and ce-

sium clusters. Therefore, in the dynamical treatment, the large number of nuclear degrees of freedom is reduced to the relative position of the projectile with respect to the centre of the cluster, \mathbf{R} . These methods have provided reasonable descriptions of electronic transitions in ion-cluster collisions for clusters of medium and large size. In the second category, all the nuclear degrees of freedom are included. This has been recently achieved (Saalman and Schmidt, 1996, 1998) through a method that combines self-consistently an MD description of the nuclear motion and a time-dependent density functional theory of the electronic degrees of freedom. This is a very promising area of research, but, to date, it has been only applied to the study of very small clusters (typically including less than 10 atoms).

Jellium Models

The jellium model is a useful approximation when the collision time is much shorter than the nuclear vibrational periods in the cluster. Indeed, in this circumstance, the cluster nuclei remain fixed in space during the collision, so that one can neglect its detailed internal structure. In addition, for short enough collision times one can apply time-dependent theories where the projectile motion is treated semiclassically. In this case, \mathbf{R} is the only nuclear degree of freedom that must be considered. Therefore, the semiclassical theory of ion-cluster collisions does not differ significantly from that of ion-atom and ion-molecule collisions. However, at variance with the latter cases, it is extremely difficult to obtain a set of correlated electronic wave functions of the ion-cluster compound system to be used in close-coupling expansions of the time-dependent wave function. Even a time-dependent Hartree-Fock approach is far beyond the present capabilities. For this reason, most methods make use of the independent electron approximation with different degrees of sophistication. Among them are first approximations based on the Vlasov equations (Gross and Guet, 1995). These equations govern the time evolution of the single-particle classical phase-space distribution $f(\mathbf{r}, \mathbf{p}, t)$ and are obtained as the classical limit of the time-dependent Hartree-Fock equations. They can be written

$$\left[\frac{\partial}{\partial t} + \mathbf{p} \cdot \nabla_{\mathbf{r}} + (\nabla_{\mathbf{p}} V[f]) \nabla_{\mathbf{r}} - (\nabla_{\mathbf{r}} V[f]) \nabla_{\mathbf{p}} \right] f(\mathbf{r}, \mathbf{p}, t) = 0, \quad (95)$$

where $V[f]$ is the total self-consistent potential acting on an electron of momentum \mathbf{p} at position \mathbf{r} . The initial phase-space distribution is taken as the Wigner transform of a realistic one-body quantal density matrix, e.g., the one-electron Kohn-Sham density. The numerical integration of the 6-dimensional Vlasov equation is not an easy task. For this reason, several simplifying strategies must be used, such as the so-called “test particle” method (see Gross and Guet (1995) for details). The Vlasov equation suffers from

Figure 8 Total cross sections for the following processes in $\text{C}^{4+} + \text{H}_2$ collisions: TCT (total single-charge transfer), FC (Franck-Condon result for single-charge transfer), CTB (charge transfer to bound vibrational states), VE (vibrational excitation), TD (dissociative charge transfer \equiv transfer dissociation), VD (vibrational dissociation). Taken from Errea *et al.* (1997).

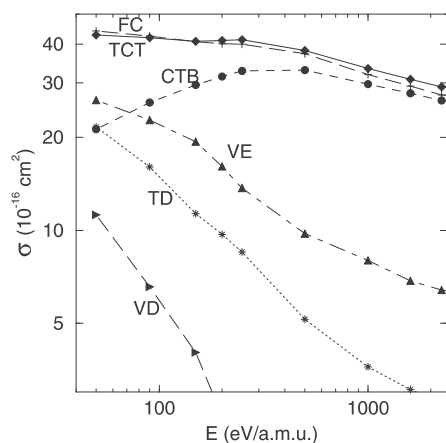
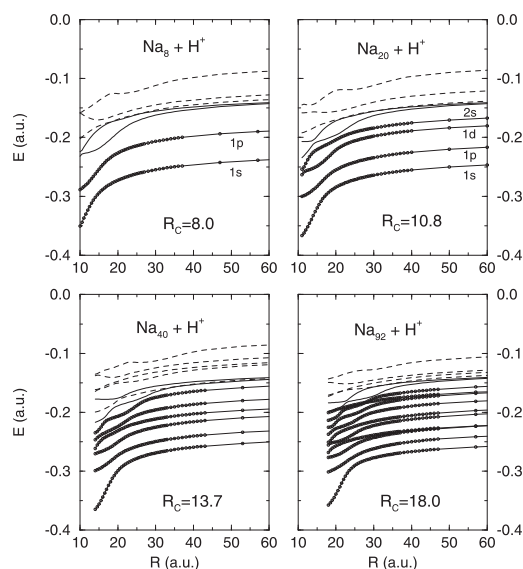


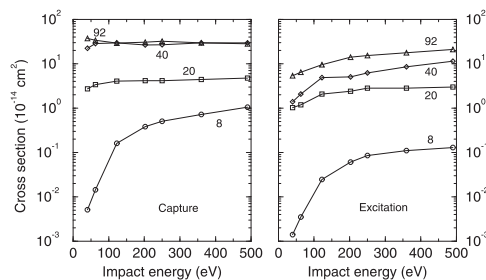
Figure 9 Potential energy curves for the σ states of the $(\text{Na}_n\text{-H})^+$ systems. Full lines, H-correlated states (capture channels); full lines with circles, occupied cluster states; dashed lines, empty cluster states. Taken from Martín *et al.* (1999a).



a severe deficiency: it does not take into account the Pauli exclusion principle. This problem is solved in practice by introducing a phenomenological exchange potential analogous to that used in the local density approximation (LDA).

Also in the framework of the independent electron approximation, a fully quantum mechanical description has been recently achieved with explicit inclusion of the Pauli exclusion principle. In this method (Martín *et al.*, 1999a), the Kohn–Sham formulation of density functional theory is used to describe the electron density of the isolated cluster in terms of single-particle orbitals. Then, from these orbitals, one obtains the corresponding one-electron potentials, V_C , including exchange, correlation and a self-interaction correction. As a consequence of the quasiseparability of the cluster Hamiltonian, the total N -electron Hamiltonian \hat{H} is then written as a sum of one-electron effective Hamiltonians, $\hat{H} = \sum_{i=1}^N \hat{h}(i)$ and thus one must only solve a set of N one-electron time-dependent Schrödinger equations. Due to the Pauli exclusion principle, the transition probability to a specific final configuration $(f_1, \dots, f_N) = \|\phi_{f_1} \dots \phi_{f_N}\|$ is written as a $(N \times N)$ determinant, $P_{f_1, \dots, f_N} = \det(\gamma_{mm'})$, where $\gamma_{mm'}$ is the one-particle density matrix, $\gamma_{mm'} = \langle f_n | \hat{\rho} | f_{n'} \rangle$, and $\hat{\rho}$ is the density operator that accounts for the time evolution of the spin-orbitals. Figure 9 shows the BO potential energy curves for the one-electron σ states of the $(\text{Na}_n\text{-H})^+$ systems. As in ion–atom collisions, transitions between different “molecular” states are induced by nonadiabatic couplings. These couplings are particularly effective in

Figure 10 Electron capture and excitation cross sections for $\text{H}^+ + \text{Na}_n$ collisions. Numbers indicate values of n . Taken from Martín *et al.* (1999b).



the vicinity of avoided crossings as those shown in Fig. 9. Thus, using these diagrams, one can explain the different electronic transitions (electron capture, excitation, ionisation, etc.) in terms of transitions between different molecular states. Figure 10 shows capture and excitation cross sections for $\text{H}^+ + \text{Na}_n$ collisions. The capture cross section is much larger than that observed in $\text{H}^+ - \text{Na}$ collisions, but the flat region is reached much earlier in the present case. It is worth noting that, at variance with ion–atom collisions, excitation cross sections are only 2–3 times smaller than electron capture cross sections. Also, multiple electronic transitions (multiple excitation, ionisation or capture) are much more important, which prevents the use of single-particle models.

More recently, some attempts have also been made in the framework of the time-dependent local density approximation. In this approximation, the electronic motion is described by the time-dependent Kohn–Sham equation in which V_C is now explicitly time dependent to take into account the response of the cluster electron density to the presence of the projectile. Although this is not strictly an independent electron model, it does not differ too much from it. Indeed, in practice, the time-dependent correlation potential is not known and approximate LDA forms must be used; since most of these forms are only justified for time-independent situations, their validity relies on the minor role played by correlation effects during the collision. Finally, it is worth mentioning a recent theoretical study of Penning detachment from negatively charged clusters (Martín *et al.*, 1999b) using the jellium approximation. The theoretical method is a combination of the semiclassical approach discussed above and the local approximation presented in section §5.

Beyond the Jellium Approximation

Recently, a nonadiabatic quantum molecular dynamics method that describes classically the motion of all nuclei (not only the projectile), simulta-

neously and self-consistently with electronic transitions, has been developed (Saalman and Schmidt, 1996, 1999). This approach has been derived on the basis of the time-dependent density functional theory, whereby the Kohn–Sham formalism within the time-dependent local density approximation is used. As an ansatz using linear combination of atomic orbitals for the Kohn–Sham orbitals a set of coupled differential equations for the time-dependent coefficients, which are used to determine the time evolution of the electronic density as the consequence of the classical atomic motion, is obtained. Simultaneously, Newton’s equations of motion with explicit time-dependent forces must be solved reflecting the possible energy transfer between the classical system of ionic cores and the quantum mechanical system of valence electrons. Thus, the nonadiabatic quantum molecular dynamics approach can be used to study both charge transfer and fragmentation processes.

References

- Bernstein, R. B. 1979, *Atom–Molecule Collision Theory*. Plenum, New York.
- Bransden, B. H. and McDowell, M. R. C. 1992, *Charge Exchange and the Theory of Ion-Atom Collisions*. Clarendon, Oxford.
- Delos, J. B. 1981, *Rev. Mod. Phys.* **53**, 287.
- Eichler, J. and Meyerhof, W. E. 1995, *Relativistic Atomic Collisions*. Academic Press, San Diego.
- Errea, L. F., Gorfinkiel, J. D., Macías, A., Méndez, L. and Riera, A. 1997, *J. Phys. B: At. Mol. Opt. Phys.* **30**, 3855.
- Errea, L. F., Gorfinkiel, J. D., Macías, A., Méndez, L. and Riera, A. 1999, *J. Phys. B: At. Mol. Opt. Phys.* **32**, 1705.
- Fritsch, W. and Lin, C. D. 1991, *Phys. Rept.* **201**, 1.
- Gross, M. and Guet, C. 1995, *Z. Phys. D* **33**, 289.
- Igarashi, A. and Lin, C. D. 1999, *Phys. Rev. Lett.* **83**, 4041.
- Kimura, M. and Lane, N. F. 1990, *Adv. At. Mol. Opt. Phys.* **26**, 79.
- Kleyn, A. W., Los, J. and Gislason, E. A. 1982, *Phys. Rep.* **90**, 1.
- Lin, C. D. 1995, *Phys. Rept.* **257**, 1.
- Martín, F. and Berry, R. S. 1997, *Phys. Rev. A* **55**, 1099.
- Martín, F. and Salin, A. 1995, *J. Phys. B* **28**, 671.
- Martín, F. and Salin, A. 1996 *Phys. Rev. A* **54**, 3990.
- Martín, F., Politis, M. F., Zarour, B., Hervieux, P. A., Hanssen, J. and Madjet, M. E. 1999a, *Phys. Rev. A* **60**, 4701.
- Martín, F., Madjet, M. E., Hervieux, P. A., Hanssen, J., Politis, M. F. and Berry, R. S. 1999b, *J. Chem. Phys.* **111**, 8934.
- Massey, H. S. W. and Smith, R. A. 1933, *Proc. R. Soc. A* **142**, 142.
- Miller, W. H. 1970, *J. Chem. Phys.* **32**, 3563.
- Pack, R. T. 1974, *J. Chem. Phys.* **60**, 633.
- Saalman, U. and Schmidt, R. 1996, *Z. Phys. D* **38**, 153.
- Saalman, U. and Schmidt, R. 1998, *Phys. Rev. Lett.* **80**, 3213.
- Sidis, V. 1990, *Adv. At. Mol. Opt. Phys.* **26**, 161.
- Sidky, E. and Lin, C. D. 1998, *J. Phys. B* **31**, 2949.
- Siska, P. E. 1993, *Rev. Mod. Phys.* **65**, 337.
- Solov’ev, E. A. 1990, *Phys. Rev. A* **42**, 1331.
- Stolterfoht, N., Dubois, R.D. and Rivarola, R. D. 1997, *Electron Emission in Heavy Ion–Atom Collisions*. Springer-Verlag, Berlin.
- Tolstikhin, O. I., Watanabe, S. and Matsuzawa, M. 1996, *J. Phys. B* **29**, L389.
- Tribedi, L. C., Richard, P., Ling, D., Wang, Y. D., Lin, C. D., Moshhammer, R., Kerby, G. W., Gealy, M. W. and Rudd, M. E. 1996, *Phys. Rev. A* **54**, 2154.
- Tseng, H. C. and Lin, C. D. 1999, *J. Phys. B* **32**, 5271.
- Weiner, J., Masnou-Seeuws, F. and Giusti-Suzor, A. 1990, *Adv. At. Mol. Opt. Phys.* **26**, 209.
- Wells, J. C., Schultz, D. R., Gavras, P. and Pindzola, M. S. 1996, *Phys. Rev. A* **54**, 593.